Low Stress Silicon Nitride Layers for MEMS Applications

Ciprian Iliescu[a], Jiashen Wei[a], Bangtao Chen[a], Poh Lam Ong[a], Francis E.H. Tay[a,b]

[a] Institute of Bioengineering and Nanotechnology, Medical Devices Group, 31 Biopolis Way, The Nanos, #04-01, Singapore 138669
[b] Department of Mechanical Engineering, National University of Singapore 10 Kent Ridge Crescent, Singapore 119260

ABSTRACT

The paper presents two deposition methods for generation of SiN_x layers with "zero" residual stress in PECVD reactors: mixed frequency and high power in high frequency mode (13.56 MHz). Traditionally, mix frequency mode is commonly used to produce low stress SiN_x layers, which alternatively applies the HF and LF mode. However, due to the low deposition rate of LF mode, the combined deposition rate of mix frequency is quite small in order to produce homogenous SiN_x layers. In the second method, a high power which was up to 600 W has been used, may also produce low residual stress (0-20 MPa), with higher deposition rate (250 to 350 nm/min). The higher power not only leads to higher dissociation rates of gases which results in higher deposition rates, but also brings higher N bonding in the SiN_x films and higher compressive stress from higher volume expansion of SiN_x films, which compensates the tensile stress and produces low residual stress. In addition, the paper investigates the influence of other important parameters which have great impact to the residual stress and deposition rates, such as reactant gases flow rate and pressure. By using the final optimized recipe, masking layer for anisotropic wet etching in KOH and silicon nitride cantilever have been successfully fabricated based on the low stress SiN_x layers. Moreover, nanoporous membrane with 400nm pores has also been fabricated and tested for cell culture. By cultivating the mouse D1 mesenchymal stem cells on top of the nanoporous membrane, the results showed that mouse D1 mesenchymal stem cells were able to grow well. This shows that the nanoporous membrane can be used as the platform for interfacing with living cells to become biocapsules for biomolecular separation

Keywords: PECVD, silicon nitride, low stress, high power, high frequency

1. INSTRUCTION

Silicon nitride (SiN_x) is one of the widely used materials in semiconductor technology, miniature devices and biomedical applications, due to its good chemical inertness, high fracture toughness, high wear resistance and biocompatibility. It can be used for passivation, insulation, mechanical protection, as well as masking layer for anisotropic etching of silicon in alkaline solutions and capping layer during implantation [1, 2]. Moreover, as membranes used in implantable microdevices and protein filtration applications which require well-controlled, stable, uniform membranes capable of biomolecular separation and minimal fouling under a wide range of biological conditions, silicon nitride received particular interest [3].

However, one critical factor which restricts its widespread use is the residual stress generated by standard processes, which is a very high tensile stress for stoichiometric silicon nitride film. The residual stress can greatly affect the device's performance, for example, the high intrinsic stress will lead to stress-induced failure via microvoid formation and structure

Micro- and Nanotechnology: Materials, Processes, Packaging, and Systems III,
edited by Jung-Chih Chiao, Andrew S. Dzurak, Chennupati Jagadish, David Victor Thiel,
Proc. of SPIE Vol. 6415, 64150L, (2006) · 0277-786X/06/$15 · doi: 10.1117/12.696350

[4,5]; the wafers will break or be severely warped if the thickness is too large. Therefore, a process that is able to generate low stress SiN_x is very important for its widespread application. On the other hand, low stress SiN_x layer has wide applications such as diaphragm in single-wafer fabricated silicon condenser microphone [6], 3-D passivation layer for planar sensors [7], hardmasks on SRAM X-ray masks [8], optical MEMS - Fabry-Pérot filter and vertical cavity surface emitting laser - [9, 10] and suspensions in micromachined silicon accelerometers [11].

In order to achieve stress reduction of SiN_x layer, several processes have been developed. Tarraf et al [12] and van de Ven et al [13] used low and high RF frequency mix, which alternatively applied low and high frequency, consequently compensating the tensile stress from high frequency (HF) by compressive stress from low frequency (LF) to produce low stress silicon nitride. Mackenzie et al [5] adjusted the stress of SiN_x through the addition of He to the standard gas mixture of SiH_4, NH_3 and N_2. By changing the ratio of N_2 and He, they achieved the stress from 300 MPa tensile through zero to about -300 MPa, compressive. Loboda and Seifferly [14] introduced Ar into the process as a diluting gas. They found that when Ar was added, $Si–H_x$ plasma chemistry and film hydrogen bond density changed, producing a reduction in the amount of tensile stress. Previous reports regarding the impact of high RF power on SiN_x layer are reported by Wu et al [15] and Sleeckx et al [16].

Here we analyze two methods to produce low stress SiN_x layers in a PECVD reactor: mix frequency method and using high power and HF mode (13.56 MHz). The paper presents the influence of the main parameters, in the fabrication of the SiN_x layers, such as: power, pressure, and SiH_4, NH_3 and N_2 flow rates. The main methods that can be used for tuning the residual stress to the desired value are also presented. Moreover, the developed SiN_x layers were tested in two MEMS fabrication processes: masking layer for wet etching in KOH and in the fabrication of a low stress cantilever by surface micromachining. Lastly, the developed technique has been used to fabricate nanoporous SiN_x membrane for cell culture system with. By cultivating D1-CDFA cells on the nanoporous membrane, it is shown that the cells can grow well on top of the silicon nitride membrane and cells isolation results are satisfying. The results mean show that the low stress SiN_x layers can be used in biomolecular separation, becoming a promising application from cellular delivery to cell-based biosensing and in vitro cell-based assays.

2. EXPERIMENTAL PROCEDURE

The deposition of SiN_x layers were performed using a plasma-enhanced chemical vapor deposition (PECVD) system (STS, Multiplex Pro-CVD). A schematic diagram of the equipment was presented by Chung et al in [17]. The unique characteristic of the system is that the plasma can be activated in two RF modes: at 380 kHz (LF) and/or at 13.56 MHz (HF). Another important characteristic of the equipment is that it offers the opportunity of selecting the power in a large range: between 0 and 600W for HF mode and between 0 and 1 kW for LF mode. The depositions of the layers were performed using pure silane (SiH_4), ammonia (NH_3) and nitrogen (N_2). To avoid contamination of the deposited layer a predisposition of a SiN_x layer was performed each time after the plasma cleaning process (usually performed after a cumulative deposition thickness of 6 μm).

For characterization of the deposited layers 4” silicon wafers, p-type, <100> crystallographic orientation, 1-10 Ωcm were used. The wafer was initially cleaned in piranha (H_2SO_4: H_2O_2 in the ratio of 2:1) at 120^{o}C for 20 minutes, rinsed in DI water and spun-dried. The native oxide of the layer was removed by dipping the wafer for one minute in a classical BOE solution. The stress characterization of the SiN_x films was performed with a stress measurement system (KLA Tencor FLX-2320). The thickness of the films was measured with a refractometer (Filmetrics F50).

3. FABRICATION OF LOW STRESS SiN_x LAYER BY MIX FREQUENCY

3.1 Deposition of SiN_x layers at low power in HF and LF mode

In most applications of PECVD, the HF (13.56MHz) RF is the most common operation mode to deposit SiN_x film. The first deposition layers were fabricated at HF and the deposition power was changed from 20W to 80W, keeping the flow rates constant as follows: $SiH_4/NH_3/N_2$ = 120/100/2200 sccm. The variations of residual stress and deposition rate of SiN_x layers at the above-mentioned range of power are shown in Figure 1. As shown the deposition rate increases with RF power. The increased RF power leads to higher electron density and therefore there is a relatively larger population of high-energy electrons. These high-energy electrons yield a higher ionization and dissociation rate, which consequently results in a higher deposition rate [18]. Moreover, the power played an important role in determining the dominant film content [21] - the layers deposited in high power process have a closer composition with the substrates due to the high dissociation rate of gases, which lead to more N+ species generated and consequently result in increased incorporation of N bonding in the SiNx film. This results in compressive stress due to the volume expansion of the SiN_x film [5]. Therefore, higher power brings high N bonding in the SiN_x film, and the higher volume expansion of the SiN_x film brings higher compressive stress, which compensates the tensile stress of the whole layer and leads to overall lower tensile stress. The result is that the deposition in HF mode, at low power (20-80 W), generates a tensile stress in the range of 120-150 MPa, the stress slowly decreases with the increasing of RF power, while the deposition rate presents a strong variation from 20W (around 15 nm/min) to 80W (around 70 nm/min).

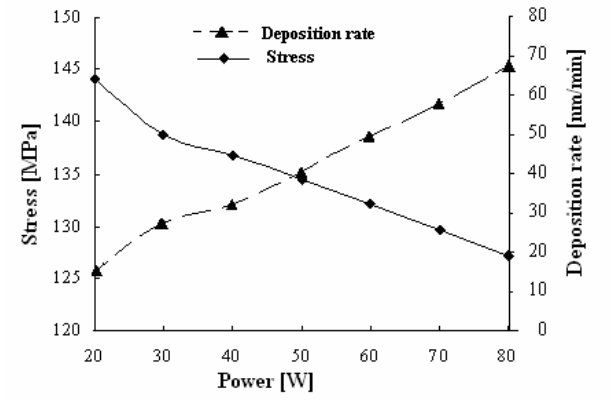

Fig 1. Variation of the stress and deposition rate of SiN_x layer at low power in HF mode (13.56 MHz)

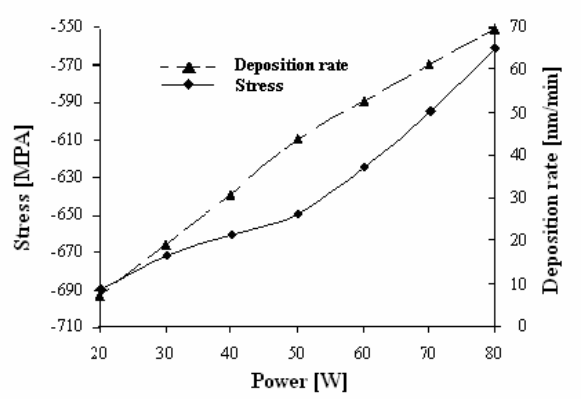

Fig 2. Variation of the stress and deposition rate of SiN_x layer at low power in LF mode (380 KHz)

Figure 2 shows the stress and deposition rate of SiN_x layers deposited using LF mode for a range of power between 20 W and 80 W. The flow rates were similar as in the previous experiment ($SiH_4/NH_3/N_2$ = 120/100/2200 sccm). It is noted that for the LF deposition mode, the intrinsic stress state of the silicon nitride layer is compressive. The main reason is that at high frequency (13.56 MHz) only the electrons are able to follow the RF field while the ions are "frozen" in place by their heavier mass. The crossover frequency at which the ions start following the electric field is between 1 and 5 MHz depending upon the mass of ions. Consequently, below 1 MHz, the ion bombardment is significantly higher, which not only enhance chemical reactions but also causes a low energy ion implantation that densifies the film and leads to a change of the stress state from tensile to compressive [13, 18, 21]. However, from Figure 2, it can be seen that the RF power has little effect on SiN_x layer stress as an increase in ion bombardment is canceled out by a higher deposition rate. We can conclude that the deposition at LF and low power (20-80 W) results in a high value of compressive stress (600-700 MPa) while the deposition rate is increasing with the power (from 7.3 nm/min at 20W to around 70 nm/min at 80W).

By alternating depositions in HF mode and LF mode or by using simultaneous both HF and LF mode we can achieve SiN_x layers with "zero residual stress". The main disadvantage of such deposition is that, in order to achieve a homogenous layer, the thickness of the compressive and tensile layer must be as thin as possible. As a result a deposition at a low power (20 - 40 W) is desired. A characteristic of low power depositions, as we have previously shown, is low deposition rate.

4. FABRICATION OF LOW STRESS SiN_x LAYER AT HIGH POWER IN HF MODE

4.1 Deposition at high power in HF mode

The observation that in HF mode the tensile stress decreases with the RF power while the deposition rate is significantly increased was further investigated in order to achieve a SiN_x layer with low stress (if it is possible, even "zero stress") and high deposition rate. A series of experiments which deposited SiN_x layer in the power range of 100 W to 600 W have been completed. Figure 3 and Figure 4 show the variations of residual stress and deposition rate respectively with the power change. In these experiments, the pressure and temperature were kept constant at 900 mTorr and 300°C respectively while several SiH_4/ NH_3/ N_2 compositions were tested: 120/75/1200 sccm, 100/60/1500 sccm and 80/60/1700 sccm.

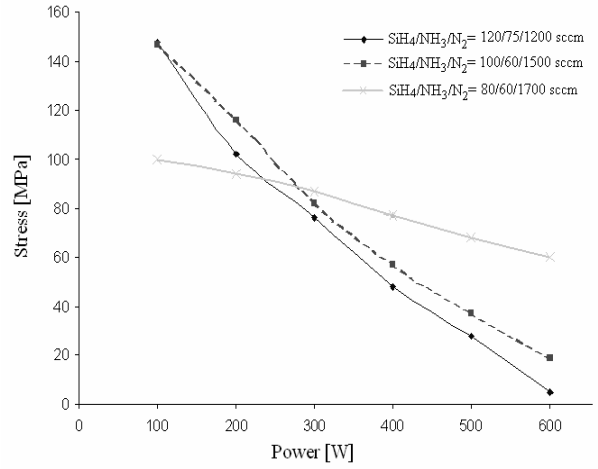

Fig 3. The change of SiN_x layer stress with the power in high power range for different $SiH_4/NH_3/N_2$ compositions

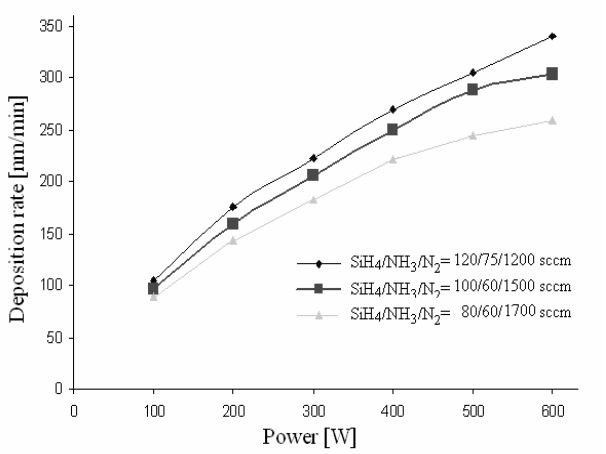

Fig 4. The change of SiN_x layer deposition rate with the power in high power range for different $SiH_4/NH_3/N_2$ compositions

From the graphs, it can be observed that, with the increase of power from 100 W to 600 W, the deposition rate increases strongly from around 100 nm/min up to 250-320 nm/min while the residual stress decreases from 100-150 MPa tensile to 4-60 MPa. It can also be noticed that the variations of the deposition rate and residual stress are strongly correlated with the composition of the mixture gas (this aspect will be presented in the next sections). For an increased concentration in SiH4 the deposition rate increases faster while the residual stress presents an accentuated decrease.

The higher power enhanced the plasma in the chamber, which subsequently yielded higher energy electrons. The increased energy of the electrons increases the dissociation of the main gases and as a result the deposition rate increases. For the

$SiH_4/NH_3/N_2$ process, the most important RF plasma-generated reactions are given by:

$$N_2 + e^- \rightarrow 2N + e^-$$

$$SiH_4 + e^- \rightarrow SiH_2 + H_2 + e^-$$

$$NH_3 + e^- \rightarrow NH_2 + H + e^-$$

Moreover, the dissociation energy of N_2 is about 9.8 eV, whereas the bond-strength H-NH_2 is only about 4.6 eV, and the critical power to activate NH_3 is only about 1/5 of that needed to activate N_2 [20]. Therefore, in the ultra high power range, much more N_2 have been activated and dissociated, which means more N atom will react with SiH_4 and much more SiN_x will be generated.

As previously explained, the decreasing stress value with the increase of power can be attributed to the high dissociation of N_2 which led to more N species and resulted in an increased of N – Si bonding in SiN_x film.

It is found that the residual stress of SiN_x layer decreases and the deposition rate increases with the increase of power. Moreover, the residual stress of silicon nitride layer deposited under the ultra high power condition (600 W) can reach a low value (4 MPa) and is strongly related to the composition. As for deposition rate, high values in the range of 250 to 320 nm/min were achieved. With increasing power, the uniformity of the deposition decreases (usually less than 2%).

4.2 Influence of NH_3 flow rate

In order to investigate the variations of residual stress and deposition rates of SiN_x layer with the NH_3 flow rate, the flow rate was varied from 45 sccm to 100 sccm. During these experiments, the SiH_4 and N_2 flow rate were kept constant at 120 sccm and 2200 sccm respectively as well as the deposition temperature (300^{o}C), the pressure (900 mTorr) and the HF mode power (600W). The results were shown in Figure 5. It can be seen that the deposition rate increases when the NH_3 flow rate decreases. Figure 5 indicates that the higher NH_3 flow rate yields higher residual stress. This is because in ultra high power range, both SiH_4 and NH_3 become activated, and when there is also sufficient excess NH_3, almost all of the SiH_4 react with it to form tetra-aminosilane, $Si(NH_2)_4$, and the triaminosilane radical, $Si(NH_2)_3$. The latter is the dominant precursor species for film growth. It decomposes on the surface and in a "condensation zone" beneath the surface in a process whereby an NH_2 and an H from neighboring precursor radicals combine to form an NH_3 molecule, which is evolved into the plasma [20]. The resulting Si and N dangling bonds pull together to propagate the Si-N network, and this generate the tensile stress. On the other hand, low NH_3 flow rate will result in "Si-rich" SiN_x layer and the high silicon content yields lower stress level [22]. Therefore, higher NH_3 flow rate leads to higher tensile stress. The decreasing of the deposition rate with the increasing of NH_3 flow rate can be explained by the cumulative effect of decreasing the number of Si species in the plasma that generates also a decreasing of $Si(NH_2)_3$ – the film growth precursor. Similar results were achieved when the deposition power was changed. In addition Lee et al reported in [23] the decrease of the deposition rate with the NH_3/SiH_4 ratio. Another interesting aspect is that the NH_3 flow rate presents a strong influence in the uniformity of the layer. For a high flow rate of NH_3 (100%) the achieved uniformity was between 1.5 to 3% while for low flow rates the uniformity was larger than10%.

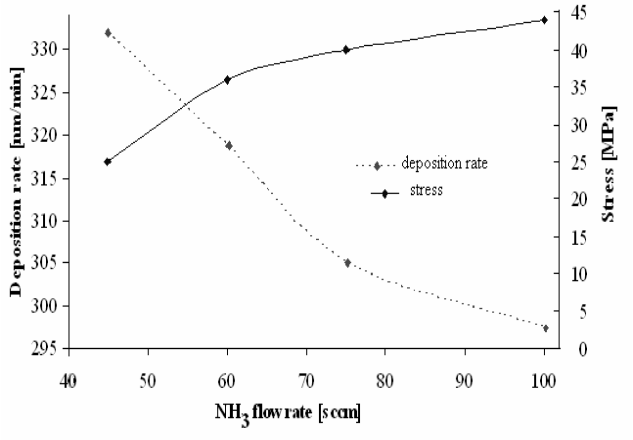

Fig 5. The change of SiN_x layer residual stress and deposition rate for high power (600 W) in HF mode under different NH_3 flow rates

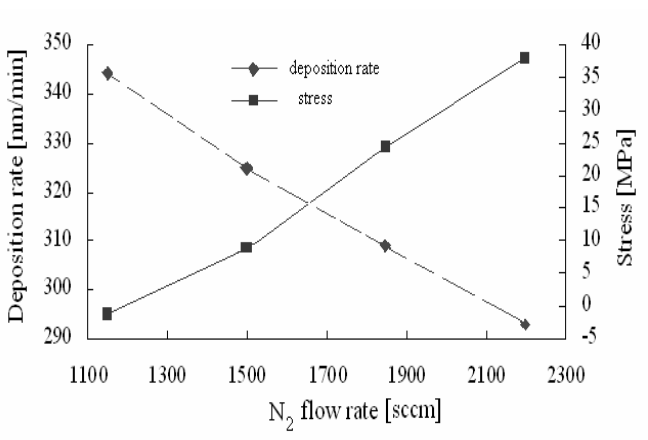

Fig 6. The change of SiN_x layer residual stress and deposition rate for high power (600 W) in HF mode under different N_2 flow rates

4.3 Influence of N_2 flow rate

Considering that N_2 also supplies the N atom for reaction, the decrease of the N_2 flow rate will lead to "Si-rich" SiN_x layer which has lower residual stress. Therefore, decreasing N_2 flow rate may produce SiN_x layer with near zero stress. In this part, the flow rates of nitrogen have been changed from 1150 sccm to 2200 sccm with the power set to be constant at 600 W to investigate the variations of deposition rate and residual stress. The flow rates of SiH4 and NH3 were 120 sccm and 75 sccm, respectively, and the pressure was set to be 900 mTorr.

Figure 6 shows how the deposition rate and stress change with N_2 flow rate. From the graph, it can be observed that the deposition rate increases and the residual stress decreases as the N_2 flow rate decreases from 2200 sccm to 1150 sccm. The drastically decreasing N_2 flow (which is much higher than the NH_3 and SiH_4 flows) has a huge impact decreasing the total gas flow rate (from 2395 to 1345 sccm). With the pressure constant, the residence time of the gas in the chamber increases. A longer residence time results in a higher dissociated rate of ammonia in the plasma with the effect of increasing of the deposition rate. Moreover, from the figure, the stress of the lowest N_2 flow rate was compressive (negative value). There were no significant influence of N_2 flow rate to the deposition uniformity, only for low flow rate (1150sccm) and increased value of uniformity was noticed.

4.4 Influence of SiH_4 flow rate

The influence of SiH_4 flow rate is presented in Figure 7. For this test, the SiH_4 flow rate was altered between 70 and 120 sccm, while NH_3 and N_2 were kept constant at 60 sccm and 1500 sccm. By increasing the SiH_4 flow rate, an increase number of Si-based radials are generated in the plasma with the effect of increasing of the deposition rate. In the mean time, the deposited SiN_x layer will be "Si rich" and as a result the stress decreases with the increasing of SiH_4 flow rate. It can be noted that with the increase of SiH_4 at 120 sccm, the resultant stress in the layer is around 13 MPa tensile, while the deposition rate increased up to 340 nm/min. No significant modification of the uniformity of the deposition with the SiH_4 flow rate was noticed (a slow increased value for SiH_4 flow rate value of 60 sccm).

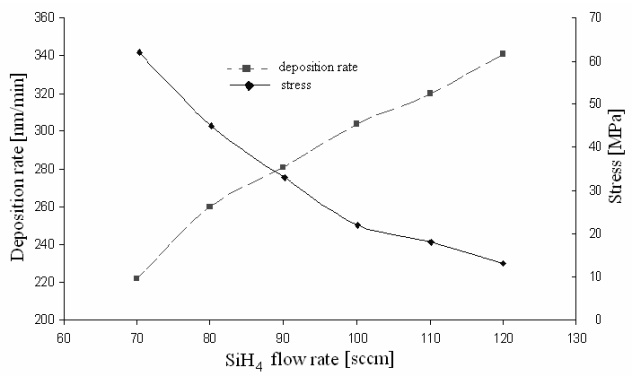

Fig 7. The change of SiN_x layer residual stress and deposition rate for high power (600 W) in HF mode under different SiH_4 flow rates

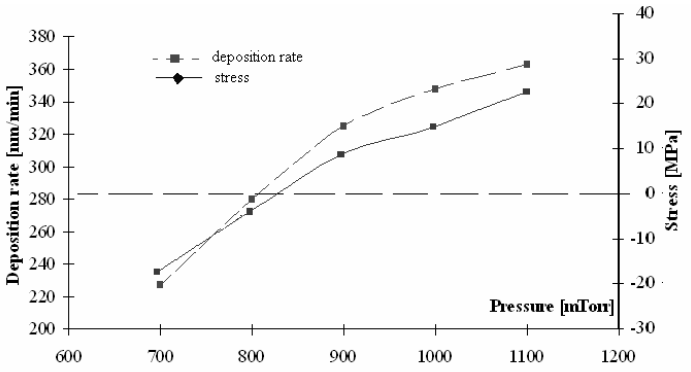

Fig 8. Variation of residual stress and deposition rate for high power (600 W) in HF mode in SiN_x layer with pressure

4.5 Influence of pressure

Pressure is another critical parameter which will greatly influence the characteristic of SiN_x layers. In this part, a series of SiN_x layers were deposited under different pressures from 700 mTorr up to 1100 mTorr, whilst other parameters were kept constant: SiH_4: 120sccm; NH_3: 75sccm; Power: 600W; N_2: 1150 sccm. Figure 8 shows how the deposition rate and residual stress changed with pressure. These two graphs indicate that pressure has a great effect on the SiN_x deposition rate and stress. The reason may be that the decreasing pressure results in an increase in electron energy, which subsequently leads to an increase in N to SiH_3 radical ratio, namely the decrease of Si/N ratio. This interpretation is consistent with the enhanced concentration of N-H bonds resulting from a pressure decrease [21]. Moreover, pressure has a great influence on plasma stabilization [20]. Therefore, from the graphs, it can be seen that at 700 mTorr pressure, the deposition rate and stress change coming from N_2 flow rate are larger than the other two. Furthermore, the uniformity of 700 mTorr is typically up to 10%, larger than those of 900 and 1100 mTorr, which are 2% and 1% respectively. However, in the 1100 mTorr pressure, the residual stress is higher. It can be concluded from the above analysis that a pressure around 900 mTorr would be optimal for SiN_x deposition due to its stable plasma and low residual stress generated.

5. MEMS APPLICATIONS

The selection of the composition of the gas flow must be performed according to the application. If we intend to deposit a masking layer for anisotropic wet etching of silicon in alkaline solution (KOH for example) a layer with low content in silicon is desired. In addition, in this case, the low value of stress is not critical. For this reason the flow rate of the SiH_4 must be reduced when compared to the flow rate of NH_3 and N_2. A composition $SiH_4/NH_3/N_2$ of 40/60/1500 sccm was selected. The resultant etching rate of SiN_x layer in 30% KOH solution at 90^{o}C was 17 nm/hour, which is similar to the etching rate of SiN_x layer deposited in LPCVD furnace. For an increased flow rate of SiH_4 at 50 sccm and 60 sccm we noticed an increased etching rate at 34 and 54 nm/hour respectively (the layer became "Si-rich" SiN_x).

Other applications require fabrication of low stress cantilevers or membranes. In this case, a low stress value is absolutely necessary. For this application a gas mixture SiH_4/ NH_3/ N_2 of 120/75/1200 sccm was used. The deposition was performed

under similar conditions: power 600W, temperature 300°C and a pressure of 850 mTorr. The resultant stress was 4 MPa tensile. The thickness of the SiN_x layer was around 1μm. A photoresist mask was applied using AZ4620 positive photoresist (from Clarian). The SiN_x layer was patterned in an ICP deep RIE AMS 100 – DE (Adixen) using CHF_3/O_2. In the next step, anisotropic etching with a Bosch process was performed in an ICP deep RIE AMS 100 - Si using the photoresist mask, up to 50μm deep, followed by the removal of the photoresist mask in an O_2 plasma in the same system. In the last step the SiN_x cantilever was released in a 30% KOH solution at 80°C. The results are presented in Figure 9 where optical and SEM images of a fabricated cantilever are presented. It can be noted that there is no bending of the cantilever which confirms the low value of the residual stress in the SiN_x layer.

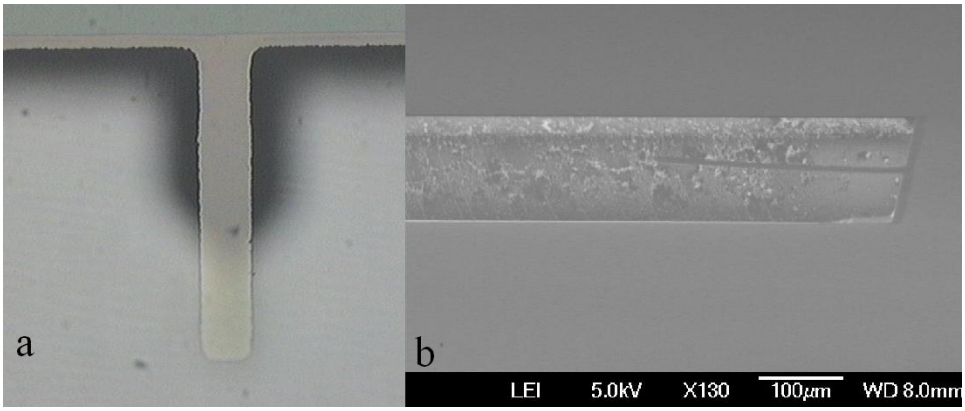

Fig 9. Optical image (a) and SEM picture (b) of the cantilever fabricated by surface micromachining

6. NANOPOROUS MEMBRANE FABRICATION AND CELL CULTURE

6.1 Nanoporous Membrane Fabrication Process

The nanoporous membranes have been fabricated by using the process shown in Figure 10. A 4" silicon wafer, <100>, p type, 1-10 Ωcm, was cleaned in piranha solution (H_2SO_4/H_2O_2 in ratio of 2:1) at 120°C for 20 minutes and then rinsed in DI water and spun-dried. Two layers of 1μm thick SiN_x layer were deposited on both sides of the two-side-polished silicon substrate based on the former optimized SiN_x deposition recipe to achieve low stress, using a STS Multiplex ProCVD System (Figure 10a). By using photolithography and an ICP deep RIE AMS 100 – DE (Adixen) system, windows on the backside are opened and an array of filter holes with 2μm radius have been patterned on the front side of the wafers (Figure 10b). For the front side of the wafer, the Deep RIE process of SiN_x etching was critical. The process was performed using $CHF_3/CH_4/O_2$ gases at a coil power of 2500W and platen power of 100W. By adding CH_4 in the classical etching process with CHF_3/O_2, the passivation of the walls increases. Next, the wafer was put into the one side-etching holder and then dipped into potassium hydroxide solution (KOH 20 %) at 90°C until about 50μm thick silicon substrate is left (Figure 10c). the process was performed with a mechanical protection of the front side of the wafer. Then the full wafer was dipped and etched in the same KOH solution at 70°C (for a better protection of the thin SiN_x membrane) to remove the remaining silicon substrate (Figure 10d). Finally, the dimension of the filter-holes was adjusted with second deposition of SiN_x layer (Figure 10e). Therefore, the holes have the radii around 400 nm, which can be seen in the SEM pictures shown as Figure 11 Moreover, from the figure, we can see that the thicknesses of horizontal and vertical surface are different which is due to the ratio between the deposition on the horizontal and vertical surface as 2:1.

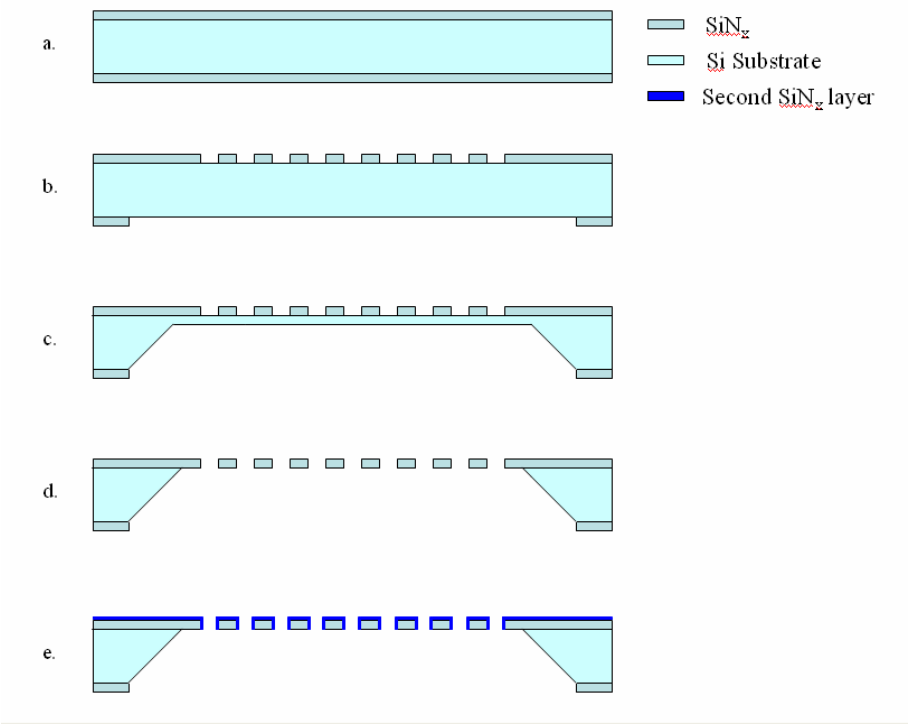

Fig 10. Fabrication process for the nanofilters. (a. SiN_x Deposition on the both sides; b. Feature patterned on the both sides; c. Single side KOH etching; d. Both side KOH etching; e. Adjust the holes)

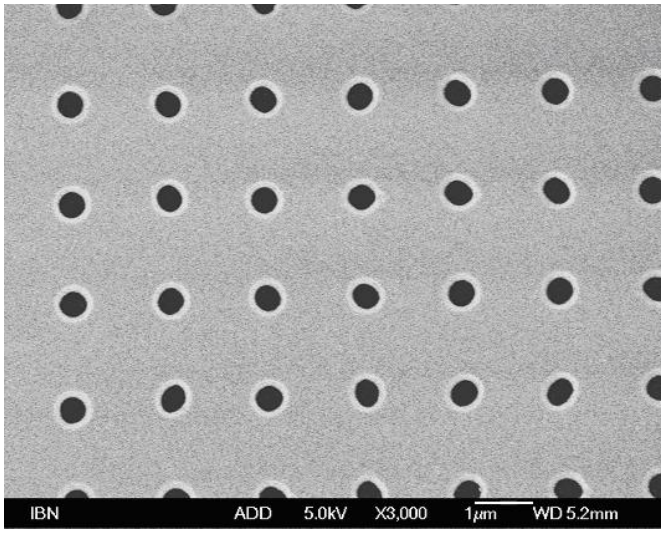

Fig 11. The SEM picture of the nanoofilters with 400nm pore size

6.2 Cell cultures

We tested the biocompatibility of the nanoporous SiN_x membrane in an in vitro cell attachment assay with the mouse D1 mesenchymal stem cells as the model cell line. Cells were stained with the cell tracker dye CFDA SE (Molecular Probes, Invitrogen) for easy visualization. Twenty-four hours after cell seeding, cells were found to adhere strongly onto the nanoporous SiN_x membrane, which can be seen from Figure 12. The picture shows the mouse D1 mesenchymal stem cells adopting a normal spread out morphology on the porous support.

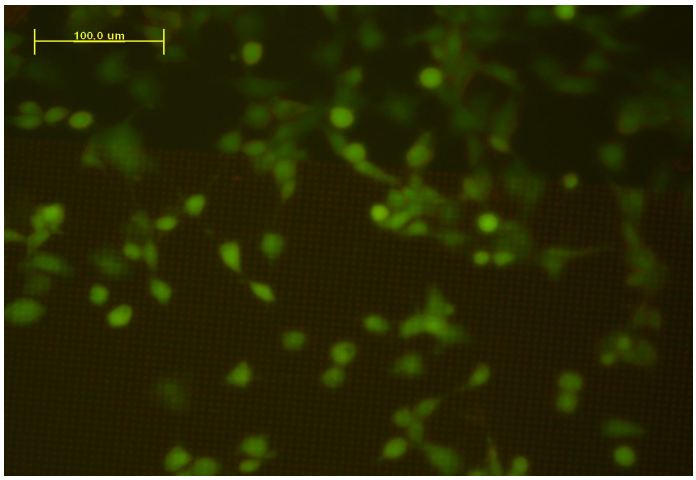

Fig 12. Mouse D1 mesenchymal stem cells with the cell tracker dye CFDA SE

By using the nanoporous membrane fabricated by stress controlled silicon nitride membrane, a micromachined membrane-based biocapsule with pore size precisely controlled can be expected, which allows free exchange of nutrients, waste products, and secreted therapeutic proteins between the host and encapsulated cells, but excludes lymphocytes and antibodies that may attack foreign cell. Microfabricated inorganic encapsulation devices by silicon nitride membrane may provide biocompatibility, in vitro chemical and mechanical stability, tailored pore geometries, and superior immunoisolation for encapsulated cells over conventional encapsulation approaches. By using microfabrication techniques, structures can be fabricated with spatial features from the sub-micro range up to several millimeters. These multi-scale structures correspond well with hierarchical biological structure, from proteins and sub-cellular organelles to the tissue and organ levels.

7. CONCLUSIONS

This paper presented two methods for the fabrication of low stress SiN_x layer in PECVD systems. One produced low stress SiN_x layer with low frequency and high frequency mixture deposition mode; the other generated the depositions at high power (600W) in HF mode (13.56 MHz). The achieved value of the residual stress was usually in the range of 0-20 MPa. Meanwhile, the latter method achieved a high deposition rate between 250 and 350 nm/min, which is much higher than the mix frequency method. Moreover, the paper analyzed other parameters that can influence the residual stress and deposition

rate such as: pressure, SiH_4, NH_3 and N_2 flow rates. The fine-tuning of residual stress can be achieved by the modification of gases flow rate or pressure. The main parameters that present a strong influence on the deposition uniformity are the NH_3 flow rate and the pressure. The paper also presented two successful applications of the SiN_x layer deposited at high power (600W) in HF mode: masking layer for anisotropic wet etching in KOH solution (an etching rate of 17nm/hour was achieved) and fabrication of a low stress SiN_x cantilever. Lastly, by using the optimized recipe, nanoporous membrane has been fabricated to present uniform and well controlled pore size as small as near 400 nm. Moreover, cultivating the mouse D1 mesenchymal stem cells on top of the nanoporous membrane, it was found that mouse D1 mesenchymal stem cells were able to grow well, which shows that the nanoporous membrane can be used as the platforms interfacing with living cells to be biocapsules which allow biomolecular separation and immunoisolation.

REFERENCES

1. Lee J Y M., Sooriakuma K, Dange M M 1991Thin Solid Films 203 275-87.
2. Neumann A, Reske T, Held M, Jahnke K 2004 J. Mater. Sci.: Mater. Med. 15 1135-40.
3. T.A. Desai, D.J. Hansford, L. Leoni, M. Essenpreis, M. Ferrari, Biosensor & Bioelectronics 15, 453 (2000).
4. K.J.Winchester, J.M.Dell, Journal of Micromechine & Microengineering 11, 589 (2001).
5. Machenzie K D, Reelfs B, DeVre M W, Westerman R, Johnson D J 2004 Chip 10, 26-9.
6. Scheeper P R, Olthuis W, Bergveld P 1994 Sensors and Actuators A 40 179-86.
7. Schmid P, Orfert M, Vogt M 1998 Surface and Coating Technology 98 1510-17.
8. Dauksher W J, Resnick D J., Smith S M., Pendharkar S V, Tompkins H G., Cummings K D, Seese P A., Mangat P J S, Chan J A 1997 J. Vac. Sci. Technol. B 15 2232-7.
9. Chitica N, Strassner M, Daleiden J 2000 Appl. Phys. Lett. 77 202-4.
10. Gukel H, Burnst D, Rutigliano C, Lovell E, Choi B 1992 J. Micromech. Microeng. 2 86-95.
11. Lapadatu D, Pyka A, Dziuban J, Puers R 1996 J. Micromech. Microeng. 6 73-6.
12. Tarraf A, Daleiden J, Irmer S, Prasai D, Hillmer H 2004 J. Micromech. Microeng. 14 317-23.
13. van de Ven E P, Connick I W, Harrus A.S 1990 Proc. of the VLSI Multilevel Interconnection Conference (VMIC), Santa Clara, CA, 94-101.
14. Loboda M J, Seifferly J A, 1996 J. Mater. Res. 11 391-8.
15. Wu T H T, et al 1992, Solid State Technology 65
16. Sleeckx E, Schaekers M., Shi X., Kunnen E, Degroote B, Jurczak M, de Potter de ten Broeck M, Augendre E 2005, Microelectronics Reliability 45 865-8.
17. Chung C K, Tsai M.Q, Tsai P H, Lee C 2005 J. Micromech. Microeng. 15/1 136-42.
18. Yan M, Geodheer W J 1999 Plasma Sources Science & Technology 8, 349.
19. Kim B, Hong W S 2004 IEEE Transactions on Plasma Science 32/1 84-9.
20. Smith D L, Alimonda A S, von Preissig F J 1990 J. of Vacuum Science & Technology B: Microelectronics 8 551-7.
21. Hess D W 1984 Journal of Vacuum Science and Technology A 2 244-52.
22. Vossen J L 1979 Journal of the Electrochemical Society 126 319-24.
23. Lee J Y M, Sooriakumar K, Dange M M 1991, Thin Solid Films 203 275-87.